Arginine Depletion Therapy with ADI-PEG20 Limits Tumor Growth in Argininosuccinate Synthase–Deficient Ovarian Cancer, Including Small-Cell Carcinoma of the Ovary, Hypercalcemic Type

Jennifer X. Ji[1], Dawn R. Cochrane[2], Basile Tessier-Cloutier[1], Shary Yutin Chen[2], Germain Ho[2], Khyatiben V. Pathak[3], Isabel N. Alcazar[3], David Farnell[1], Samuel Leung[4], Angela Cheng[4], Christine Chow[4], Shane Colborne[5], Gian Luca Negri[5], Friedrich Kommoss[6], Anthony Karnezis[7], Gregg B. Morin[5,8], Jessica N. McAlpine[9], C. Blake Gilks[1], Bernard E. Weissman[10], Jeffrey M. Trent[11], Lynn Hoang[1], Patrick Pirrotte[3], Yemin Wang[2], and David G. Huntsman[1,2,9]

ABSTRACT

Purpose: Many rare ovarian cancer subtypes, such as small-cell carcinoma of the ovary, hypercalcemic type (SCCOHT), have poor prognosis due to their aggressive nature and resistance to standard platinum- and taxane-based chemotherapy. The development of effective therapeutics has been hindered by the rarity of such tumors. We sought to identify targetable vulnerabilities in rare ovarian cancer subtypes.

Experimental Design: We compared the global proteomic landscape of six cases each of endometrioid ovarian cancer (ENOC), clear cell ovarian cancer (CCOC), and SCCOHT to the most common subtype, high-grade serous ovarian cancer (HGSC), to identify potential therapeutic targets. IHC of tissue microarrays was used as validation of arginosuccinate synthase (ASS1) deficiency. The efficacy of arginine-depriving therapeutic ADI-PEG20 was assessed *in vitro* using cell lines and patient-derived xenograft mouse models representing SCCOHT.

Results: Global proteomic analysis identified low ASS1 expression in ENOC, CCOC, and SCCOHT compared with HGSC. Low ASS1 levels were validated through IHC in large patient cohorts. The lowest levels of ASS1 were observed in SCCOHT, where ASS1 was absent in 12 of 31 cases, and expressed in less than 5% of the tumor cells in 9 of 31 cases. ASS1-deficient ovarian cancer cells were sensitive to ADI-PEG20 treatment regardless of subtype *in vitro*. Furthermore, in two cell line mouse xenograft models and one patient-derived mouse xenograft model of SCCOHT, once-a-week treatment with ADI-PEG20 (30 mg/kg and 15 mg/kg) inhibited tumor growth *in vivo*.

Conclusions: Preclinical *in vitro* and *in vivo* studies identified ADI-PEG20 as a potential therapy for patients with rare ovarian cancers, including SCCOHT.

Introduction

Ovarian cancer is the fifth most common cause of cancer death in women, accounting for more than 22,240 new diagnoses and 14,070 deaths in the United states in 2018 (1). Ovarian cancer can be categorized into epithelial cancers which mostly include high-grade serous (HGSC), endometrioid (ENOC), and clear cell ovarian carcinomas (CCOC), and nonepithelial cancers that arise from ovarian germ cells, sex cord cells, stromal cells, or have unknown origin. Each subtype has unique histologic and molecular characteristics with distinct cells of origin, suggesting that they are and should be managed as different diseases (2). Nonetheless, standard-of-care for all ovarian cancer subtypes, aside from surgical resection, is radiotherapy and taxane/platinum chemotherapeutics. Less common subtypes such as late-stage CCOC and small-cell carcinoma of the ovary, hypercalcemic type (SCCOHT) are often not responsive to cytotoxic chemotherapy. HGSC, the most common subtype, accounting for over 70% of all cases, has benefited from research efforts leading to the development of targeted therapeutics such as PARP inhibitors (3). However, these targeted therapeutics have limited applicability in treating patients with ovarian cancer subtypes beyond HGSC. Therefore, there is an urgent unmet need to identify novel therapeutic targets for these uncommon ovarian cancers.

While HGSC is associated with mutations in tumor suppressor *BRCA1/2* and *TP53*, both ENOC and CCOC are thought to arise from

[1]Department of Pathology and Laboratory Medicine, University of British Columbia, Vancouver, Canada. [2]Department of Molecular Oncology, BC Cancer Agency, Vancouver, Canada. [3]Collaborative Center for Translational Mass Spectrometry, The Translational Genomics Research Institute, Phoenix, Arizona. [4]Genetic Pathology Evaluation Center, Vancouver, Canada. [5]Michael Smith Genome Sciences Centre, BC Cancer Agency, Vancouver, Canada. [6]Institute of Pathology, Medizin Campus Bodensee, Friedrichshafen, Germany. [7]Department of Pathology and Laboratory Medicine, University of California, Davis, California. [8]Department of Medical Genetics, University of British Columbia, Vancouver, Canada. [9]Department of Obstetrics and Gynecology, University of British Columbia, Vancouver, Canada. [10]Department of Pathology and Laboratory Medicine, UNC–Chapel Hill, Chapel Hill, North Carolina. [11]Integrated Cancer Genomics, The Translational Genomics Research Institute, Phoenix, Arizona.

Note: Supplementary data for this article are available at Clinical Cancer Research Online (http://clincancerres.aacrjournals.org/).

Corresponding Author: David G. Huntsman, University of British Columbia, BC Cancer Research Centre, 675 West 10th Avenue, Vancouver, BC V5Z 4E6, Canada. Phone: 604-675-8205; Fax: 604-675-8214; E-mail: dhuntsma@bccancer.bc.ca

Clin Cancer Res 2020;26:4402–13

doi: 10.1158/1078-0432.CCR-19-1905

Translational Relevance

Many rare ovarian cancers lack effective management strategies and are resistant to the standard platinum- and taxane-based chemotherapy. Thus, for a rare ovarian cancer subtype like small-cell carcinoma of the ovary, hypercalcemic type (SCCOHT)—an aggressive malignancy affecting young women in their 20s—effective targeted therapeutics are urgently needed. We used global proteomics to identify a deficiency in arginosuccinate synthase (ASS1) as a common feature among some rare ovarian cancer subtypes. Using *in vitro* and *in vivo* models, we demonstrated that the arginine-depriving investigational agent ADI-PEG20 effectively inhibited cell growth in ASS1-deficient ovarian cancers, including SCCOHT, establishing it as a potential therapeutic agent for rare ovarian cancer subtypes deficient in ASS1. Further clinical investigation is warranted.

ovarian endometriosis, harboring mutations in *ARID1A*, *PIK3CA*, and *PTEN* (4, 5). ENOC has a higher incidence of *CTNNB1* mutations and mismatch repair defects compared with CCOC (6, 7). Compared with CCOC, ENOC has a less aggressive clinical course with most patients diagnosed at early stages. CCOC accounts for about 10% to 12% of all ovarian cancer cases and is considered a high-grade malignancy. While having a better prognosis when diagnosed at early stages, about 33% of patients with CCOC present at late stage, and have the worst outcome among all epithelial ovarian cancer subtypes (8). The antiangiogenesis agent sunitinib was found to have minimal activity in refractory CCOC in a phase II study (9). Further clinical research efforts evaluating agents inhibiting angiogenesis (NCT02866370) and overactive PI3K pathway (NCT01196429) in CCOC are underway with a recent focus on immunotherapy (10). Despite these advancements, effective and affordable targeted therapeutics for CCOC are still lacking.

SCCOHT is a highly aggressive cancer affecting young women, having a median age of diagnosis at 24 years old. The cellular of origin of SCCOHT remains unclear. The tumor is resistant to conventional chemotherapeutics and unfortunately, most patients succumb to their disease within 2 years of diagnosis (11). SCCOHT is characterized by a dual loss of SMARCA2 and SMARCA4, two mutually exclusive ATPases of the SWI/SNF chromatin remodeling complex (12). Notable recent development in therapeutics for SCCOHT include EZH2 inhibitor (13), HDAC inhibitor (14), ponatinib (15), and a CDK4/6 inhibitor (16) which show promising efficacy in preclinical models. Clinical translation of these molecules is highly anticipated. Targeted therapeutics should continue to be pursued for this highly aggressive cancer to maximize patient survival. Other nonepithelial ovarian cancers include granulosa cell tumor (GCT) and Sertoli–Leydig cell tumor (SLCT). Both GCT and SLCT can have an indolent course, but at late stage and upon recurrence, the outcome is poor due to the lack of response to chemotherapy (17, 18).

To identify common vulnerabilities in rare ovarian cancers to support a basket trial design, we surveyed the global proteomic landscape of CCOC, ENOC, SCCOHT, and HGSC. We identified low/absent levels of arginosuccinate synthase (ASS1) in rare cancer subtypes including SCCOHT, a portion of CCOC, ENOC, and SLCT. In HGSC, decreased ASS1 expression has been associated with platinum resistance (19). Furthermore, Cheon and colleagues reported that ASS1 protein expression by IHC overall was high in HGSC and lower in CCOC, ENOC, and mucinous cancers (20). While ASS1, the rate-limiting enzyme in intracellular arginine synthesis, is expressed in most normal tissues (21), cancers low in ASS1 are auxotrophic for arginine (22). This vulnerability has been explored by using ADI-PEG20, a PEGylated arginine deiminase effectively depleting extracellular arginine (23). ADI-PEG20 is currently under phase I to III investigation in various malignancies as a monotherapy and in combination with cytotoxic chemotherapy (22). To date, there are no clinical trials of ADI-PEG20 in ovarian cancers, possibly due to the observation that most HGSC have high ASS1 expression, but opportunities for stratification for more rare ovarian cancer subtypes remain unexplored. In this study, we showed that ADI-PEG20 is an effective therapy in preclinical models of uncommon ovarian cancer subtypes deficient in ASS1, including CCOC and SCCOHT.

Materials and Methods

Cell lines

Cell lines representing CCOC (JHOC 5, JHOC 7, JHOC 9, OVTOKO, ES2), ENOC (IGROV1), dedifferentiated ovarian cancer (TOV112D), and SCCOHT (SCCOHT1, BIN67, COV434) were grown in RPMI with 5% FBS. HGSC cell line OVCAR3 was cultured in 199/105 medium supplemented with 5% FBS. SCCOHT1 cell line was provided by Dr. Ralf Hass (24), BIN67 were provided by Dr. Barbara Vanderhyden, and COV434 cells were provided by Dr. Mikko Anttonen. JHOC 5, JHOC 7, and JHOC 9 were obtained from the RIKEN Cell Bank. ES2 and TOV112D were obtained from ATCC. IGROV1 was obtained from the NCI cell bank whereas OVTOKO was obtained from the JCRB cell bank. Cells were maintained in an incubator with 5% CO_2 at 37°C, were all short tandem repeat validated and negative for *Mycoplasma*. Early passages were used for experiments (passages 3–10 from thawing).

Proteomic analyses

Global proteomic data for six cases each of HGSC, CCOC, and ENOC were obtained from previous publication (25). An additional six cases each of SCCOHT and HGSC were analyzed using SP3-Clinical Tissue Proteomics (SP3-CTP) followed by the probe-level expression change averages (PECA) bioinformatic pipeline as described previously (25). For this analysis, two 10-μmol/L scrolls of formalin-fixed, paraffin-embedded (FFPE) tissue were used. The new cases were analyzed in two TMT-11 plexes. Each TMT plex contained a pooled internal standard (PIS) generated from pooling equal portions from each case included in this study at the peptide level. The PIS was used to normalized between plexes.

Patient cohorts

Tissue microarrays (TMA) containing FFPE CCOC ($n = 28$), ENOC ($n = 27$), HGSC ($n = 207$), SCCOHT ($n = 15$), low-grade serous (LGSC; $n = 9$), adult GCT ($n = 35$), juvenile GCT ($n = 8$), and SLCT ($n = 17$) were obtained as described previously (12, 26, 27). An additional TMA containing 16 cases of SCCOHT was obtained as described previously (28). The TMA containing endometrial endometrioid cases were included in a study by McConechy and colleagues (6) as described previously (29). An additional 67 cases of CCOC were obtained from the OVCARE tissue bank and Vancouver General Hospital (VGH) archives, subsequently reviewed by a pathologist to confirm diagnosis (B. Tessier–Cloutier, L. Hoang). An additional 28 cases of SLCT were reviewed by a pathologist (C.B. Gilks). Duplicate 0.6-mm cores from each case were used for TMA construction using a tissue microarrayer (TMArrayer by Pathology devices). The study was conducted in accordance with the International Ethical Guidelines for

Biomedical Research Involving Human Subjects (CIOMS). Informed written consent was obtained from each subject or each subject's guardian under the OVCARE tissue bank protocol approved by the research ethics board (REB; H05-60119). Use of VGH archival tissues was indicated under approved REB protocol (H02-61375).

IHC and scoring

IHC was performed on 4-μm sections using the Ventana Discovery automated stainer (Ventana Medical Systems) at the Genetic Pathology Evaluation Center. Staining was performed using antibodies to ASS1 (Rabbit polyclonal, Sigma, HPA020934), and Ki67 (Rabbit monoclonal SP6, Thermo Fisher Scientific, RM-9106-S0). For Ki67, anti-rabbit secondary antibody (Vector Biotin, Anti-rabbit, 1:300 with Discovery Diluent) was manually applied and incubated for 32 minutes then visualized with DAB detection kit. All TMAs were scored by pathologists (B. Tessier–Cloutier, L. Hoang). Histoscores were calculated by multiplying the average staining intensity (0 negative, 1 low, 2 moderate, and 3 intense) in tumor cells by percent tumor cells staining, resulting in histoscores from 0 to 300. In cases which had multiple regions represented on TMA, the highest histoscore was used. Ki67 score was determined by a pathologist (D. Farnell), and was defined as the percentage of positively staining tumor cells in the area of the most intense staining. Mitotic count was scored by a pathologist (D. Farnell) using whole H/E slides from FFPE tissue of mouse xenografts. Mitotic count per case was determined by the total mitotic figure in three high-power fields (0.237 mm^2/field), and reported as mitotic count per millimeter squared.

Cell proliferation and IC_{50} assay

Cells were seeded in 96-well plates in triplicates (3,000–5,000 cells/well, depending on cell line) and allowed to attach for 24 hours. Cells were treated with 0.63 μg/mL of ADI-PEG20 after attachment. Growth curves were monitored for 4 days by using an Incucyte ZOOM live cell imaging monitor (Essen BioScience). For IC_{50} assays, cells were seeded in 96-well plates in triplicates and allowed to attach for 24 hours. Cells were treated with 10 concentrations of ADI-PEG20 for 4 days. At the end of the experiment, cells were fixed in 10% methanol–10% acetic acid for 10 minutes and stained with 0.5% crystal violet in methanol for 10 minutes. The plates were dried overnight and dissolved in 10% acetic acid in water for 10 minutes and measured at 595 nm in a spectrometer.

Mouse xenografts

Animal care was carried out following guidelines approved by the Animal Care Committee of the University of British Columbia (Vancouver, Canada; A17-0146). PDX-465 was passaged (p13) and injected subcutaneously as described previously (15). SCCOHT cell lines COV434 and SCCOHT1 were collected in 1× Hank's Balanced Salt Solution and prepared to a final volume of 200 μL per mice with a 1:1 mixture with Matrigel (Corning). The final suspension was injected subcutaneously in the backs of 7–9-week-old female NRG (NOD.Rag1KO.IL2RγcKO) mice (2×10^6/mouse). The mice were randomized when average tumor volume reaches 100 mm^3 into saline control group and treatment groups. ADI-PEG20 (Polaris Pharmaceuticals) or saline control (200 μL) was administered via intraperitoneal injection weekly for 4 weeks. Tumor volume and mouse weight were measured three times weekly. Tumor volume was calculated as length × $(\text{width})^2$ × 0.52. At study termination, tumors were collected, weighed, and fixed in 10% formalin for 48 hours before being embedded in paraffin.

Statistical analysis

IC_{50} calculation was determined by the GraphPad PRISM software, all other statistical tests were performed in R. Statistical significance between two groups was calculated using the Student *t* test. Statistical significance between three or more groups was calculated using ANOVA with *post hoc* Tukey test when indicated. For proteomics, differential protein expression at the peptide level was obtained using PECA (25), *P* values were FDR-adjusted using the Benjamini–Hochberg procedure. Proteins with an absolute $\log_2$ fold-change > 1 and adjusted *P* value (P_{adj}) < 0.05 were considered to be differentially expressed. Multigroup comparison of expression in boxplots was investigated using Kruskal–Wallis test, with a *post hoc* Dunn test with Benjamini–Hochberg multiple testing correction. Statistical significance in pairwise expression comparison in box plots was calculated with a Whitney–Mann *U* test.

Additional methods may be found in the Supplementary Material and Methods.

Results

Global proteomics identifies ASS1 as a low abundance protein in rare ovarian cancer subtypes

To identify putative therapeutic targets unique to uncommon ovarian cancers, we analyzed the global proteomic profiles of six cases each of CCOC, ENOC, and HGSC that we have previously characterized (25) and in a separate analysis, those of additional six cases each of HGSC and SCCOHT that we have recently profiled (unpublished data, manuscript in preparation) using SP3 CTP (25). Supplementary Table S1 lists the proteins differentially expressed in two or more less common ovarian cancer subtypes when compared with HGSC. We choose to follow up on metabolic features for which therapies are in clinical development to advance targeted therapeutic in rare ovarian cancers. Differential expression analyses identified ASS1, the rate-limiting enzyme in intracellular arginine synthesis (21), as having a significantly higher protein abundances in HGSC compared with ENOC and SCCOHT ($\log_2$ fold-change = 2.2 and 2.4, respectively, $P_{adj} < 0.0001$; **Fig. 1A** and **C**) and a trend of having a higher expression in HGSC when compared with CCOC ($\log_2$ fold-change = 0.71, P_{adj} = 0.14; **Fig. 1B**). ASS1 peptides were identified in all analyzed samples with good coverage in both the original and additional proteomic sets (11 and 22 unique peptides, respectively), suggesting the differential expression of ASS1 was unlikely an artifact of mass spectrometry analysis. The protein expression *Z*-score indicated variable ASS1 protein abundance among six CCOC cases (**Fig. 1D**). In contrast, all six cases of ENOC had comparatively low ASS1 expression, and all HGSC exhibited relatively high protein abundance (**Fig. 1D**). In the HGSC and SCCOHT proteomic analysis, all but one case of HGSC had relatively high ASS1 abundance, and all six SCCOHT cases exhibited low ASS1 protein expression (**Fig. 1E**). These proteomic results suggest that while a majority of HGSC cases have high ASS1 expression, lower ASS1 expression may be a common feature among some rare ovarian cancer subtypes, including a subset of CCOC, the majority of ENOC, and all SCCOHT cases.

Varied ASS1 expression in ovarian cancer subtypes

To validate the proteomic findings, we used IHC to survey ASS1 protein expression in an extended patient cohort including epithelial and nonepithelial ovarian cancer subtypes (**Fig. 2**; **Table 1**). ASS1 exhibited cytoplasmic staining in tumor cells, some inflammatory cells, as well as endothelial cells (**Fig. 2A** and **C**). In HGSC ($n = 207$), ASS1 was highly expressed, where 178 of 207 (86%) had uniformly strong

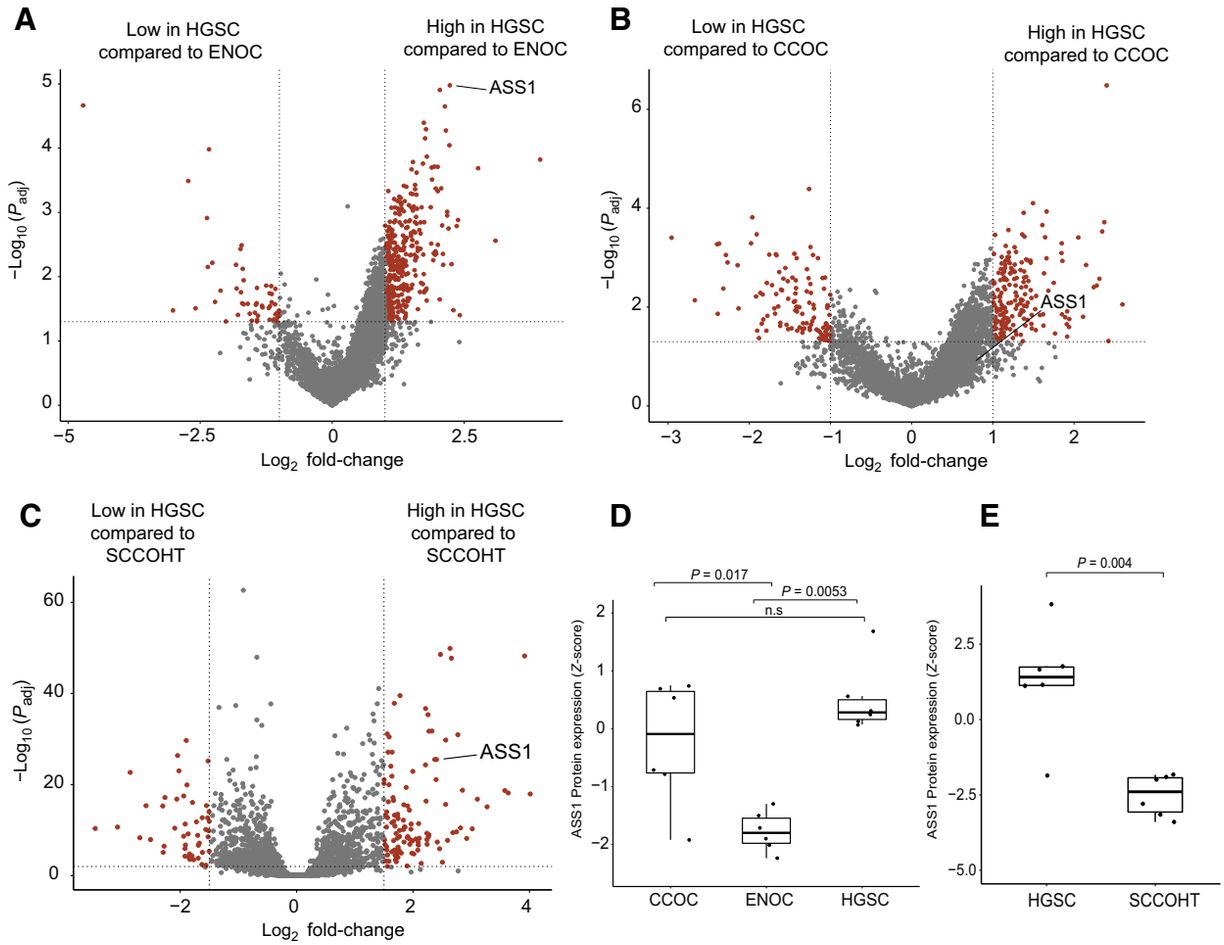

Figure 1.

Global proteomics identifies decreased ASS1 expression in rare ovarian cancer subtypes. Proteomics data for six cases each of CCOC, ENOC, and HGSC were obtained from a previous publication (25). An additional six cases each of SCCOHT and HGSC were analyzed using SP3-CTP global proteome profiling. Volcano plot showing differentially expressed proteins comparing ENOC to HGSC (**A**), CCOC to HGSC (**B**), and SCCOHT to HGSC (**C**). Significantly differentially expressed proteins are highlighted in red, and were defined as $\log_2$ fold-change larger than 1 or smaller than −1, and an FDR-adjusted $P < 0.05$. Boxplot showing ASS1 protein expression *Z*-score in each case of CCOC, ENOC, and HGSC (**D**), and SCCOHT compared with HGSC (**E**). The statistical significance in multiple group comparisons is calculated with a Kruskal–Wallis test with a *post hoc* Dunn test with Benjamini–Hochberg correction. Pairwise comparison in **E** was calculated using a Mann–Whitney *U* test.

expression with a histoscore of 300 (**Fig. 2B**). In contrast, SCCOHT had uniformly low ASS1 expression with 96.8% (30/31) of cases having a histoscore of less than 100 (median histoscore = 3.5; **Fig. 2D**). Twenty-one of 31 cases (67%) either exhibited no ASS1 expression ($n = 12$), or weak staining in less than 5% of all tumor cells ($n = 9$). For the SCCOHT cases containing mixed histologic areas of small-cell morphology, large cell morphology, and rhabdoid morphology ($n = 15$), ASS1 staining, if present, was uniform across morphologically distinct areas, suggesting homogenous expression (Supplementary Fig. S1). In CCOC ($n = 95$), 69 of 95 (72%) expressed ASS1 strongly with a histoscore of 300 while 26 of 95 (28%) cases exhibited decreased ASS1 expression (histoscore <300), including 10 of 28 (36%) patients with stage III/IV. ENOC ($n = 39$) had markedly lower protein expression (median histoscore = 100; **Fig. 2B**). When comparing high expression (histoscore = 300) to decreased expression (histoscore <300), ASS1 expression did not correlate with overall and progression-free survival in ENOC and CCOC (Supplementary Fig. S2).

We further determined ASS1 expression in a cohort of LGSC and sex-cord stromal cell tumors. LGSC cases ($n = 9$) exhibited high ASS1 expression with eight of nine cases having a histoscore of 300. In ovarian sex-cord stromal cell tumors, ASS1 expression was moderate in adult and juvenile GCTs ($n = 35$ and 8, respectively, median histoscore = 180 and 210, respectively). ASS1 expression was decreased in SLCT ($n = 45$, median histoscore = 40) with 60% having a histoscore <100 (**Fig. 2C** and **D**).

To investigate possible correlations between genomic alteration and ASS1 expression, we obtained ENOC ($n = 26$) and CCOC ($n = 35$) cases with available whole-genome sequencing and matched RNA sequencing (RNA-seq) data (30). *ASS1* mRNA expression did not correlate with *ARID1A* or *PIK3CA* mutations in CCOC and ENOC (data not shown). All eight of 26 ENOC cases with medium to high impact *CTNNB1* mutation exhibited lower *ASS1* mRNA *Z*-score (Supplementary Fig. S3A). We then assessed ASS1 expression using IHC in an extended local cohort of endometrioid ovarian and

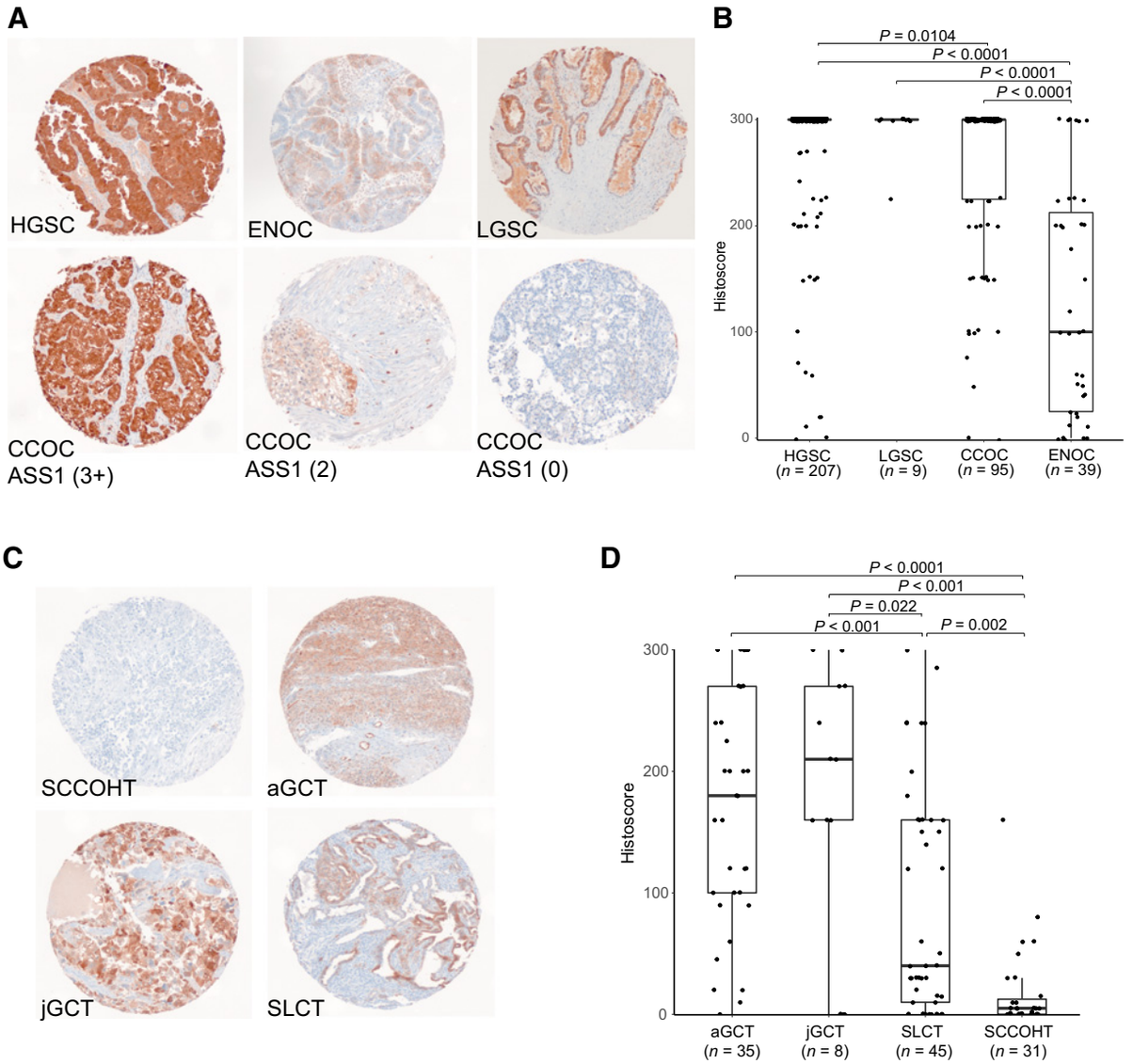

Figure 2.

ASS1 IHC demonstrates differential expression in ovarian cancer subtypes. Representative IHC stains in TMA cores of epithelial ovarian cancer subtypes, including differential expression seen in CCOC (**A**) and nonepithelial subtypes (**C**). Corresponding boxplots depicting ASS1 histoscore distribution in epithelial subtypes (**B**) and nonepithelial subtypes (**D**). Histoscore was calculated by multiplying the average staining intensity by the percentage of tumor cells staining positive. The statistical significance in multiple group comparisons is calculated with a Kruskal–Wallis test with a *post hoc* Dunn test with Benjamini–Hochberg correction.

endometrioid endometrial cancers (EEC) for which the *CTNNB1* mutation status had been determined previously (6). Findings in the extended cohort confirmed correlation between *CTNNB1* mutation and lower ASS1 protein expression in both ENOC and EEC ($P = 0.004$ and $P < 0.001$; Supplementary Fig. S3B). This correlation was further supported by an analysis using the EEC genomic and RNA-seq data from The Cancer Genome Atlas ($P < 0.001$; Supplementary Fig. S3C). To address whether ASS1 is silenced due to SMARCA4 inactivation in SCCOHT, we reexpressed SMARCA4 in three SCCOHT cell lines and did not observe any impact on ASS1 expression (Supplementary Fig. S4A).

ADI-PEG20 susceptibility is specific to ASS1 deficiency in ovarian cancers

ADI-PEG20 is a PEGylated form of arginine deiminase which effectively deprives plasma arginine. It is currently being investigated in phase I to III clinical trials targeting advanced cancers (31, 32). To assess whether ASS1-deficient ovarian cancers are sensitive to ADI-PEG20 treatment, we investigated ASS1 expression in a panel of cell lines representing a wide range of ovarian cancer subtypes. We observed ASS1 expression in the HGSC cell line OVCAR3 and differential ASS1 expression was observed in CCOC cell lines, in contrast, cell lines representing SCCOHT (BIN67, SCCOHT1,

Table 1. ASS1 histoscore in ovarian cancer subtypes.

	High-grade serous ovarian cancer	Low-grade serous ovarian cancer	Clear cell ovarian cancer	Endometrioid ovarian cancer	Adult granulosa cell tumor	Juvenile granulosa cell tumor	Sertoli–Leydig cell tumor	Small-cell carcinoma of the ovary, hypercalcemic type
Cases with interpretable ASS1	207	9	95	39	35	13	45	31
Median ASS1 score	300 (0–300)	300 (225–300)	300 (0–300)	100 (0–300)	180 (0–300)	210 (0–300)	40 (0–300)	3.5 (0–160)
ASS1 histoscore								
300	178 (86%)	8 (88.9%)	69 (72.6%)	6 (15.4%)	7 (20%)	2 (15.4%)	1 (2.2%)	0
200–285	16 (7.7%)	1 (11.1%)	10 (10.5%)	9 (23.1%)	10 (28.6%)	5 (38.5%)	6 (13.3%)	0
100–180	5 (2.4%)	0	12 (12.6%)	7 (17.9%)	10 (28.6%)	3 (23.1%)	11 (24.4%)	1 (3.2%)
10–90	6 (2.9%)	0	2 (2.1%)	11 (28.2%)	7 (20%)	0	16 (35.6%)	9 (29%)
0—5	2 (0.96%)	0	2 (2.1%)	6 (15.4%)	1 (2.9%)	3 (23.1%)	11 (24.4%)	21 (67.7%)

COV434), dedifferentiated ovarian cancer (TOV112D), and ENOC (IGROV1) did not express ASS1 (**Fig. 3A**). We then stained ASS1 on an existing TMA containing FFPE cell pellets from a panel of ovarian cancer cell lines, ASS1 IHC corresponds to ASS1 expression on Western blot analysis, supporting the utility of the antibody in an IHC capacity (Supplementary Fig. S4B). We confirmed the specificity of the antibody for IHC using FFPE pellets of isogenic overexpression and knockout cell lines (Supplementary Fig. S4C). Protein expression correlated with mRNA expression in cell lines (Supplementary Fig. S4D). While *ASS1* was silenced by promoter methylation in cancers including some HGSC (19, 33), we saw promoter methylation of *ASS1* in two of three SCCOHT cell lines, but not CCOC cell lines (Supplementary Fig. S4E). Furthermore, arginine was shown to be essential for cell survival as both ASS1-expressing cell line JHOC 7 and ASS1-deficient cell line JHOC 5 exhibited growth arrest when cultured in media lacking arginine and citrulline. Citrulline, along with aspartate, is an essential precursor for the generation of arginosuccinate by ASS1 (21). The addition of citrulline rescued the growth of JHOC 7 but not JHOC 5, indicating *de novo* arginine production is essential for ovarian cancer cell survival in arginine depleted conditions (Supplementary Fig. S4F).

ADI-PEG20 treatment was effective in inhibiting the growth of all ASS1-deficient cell lines but not ASS1-expressing cell lines (**Fig. 3B**; Supplementary Fig. S5). In a 4-day assay, ASS1-deficient ovarian cancer cell lines were extremely sensitive to ADI-PEG20 regardless of subtype with the IC_{50} ranging from 0.051 to 0.15 μg/mL, whereas cell lines expressing ASS1 were not susceptible with a calculated IC_{50} of larger than the highest concentration tested (2 μg/mL; **Fig. 3C**; Supplementary Fig. S6). To assess whether ADI-PEG20 treatment was cytotoxic, we determined the rate of apoptosis by measuring the activation of caspase 3/7 using a cell permeable dye that labels activated caspase 3/7 followed by monitoring in a live cell monitor for 3 days. Two ASS1-null cell lines, JHOC 5 and COV434, exhibited a significant increase in apoptotic tumor cells (41% and 52%, respectively) compared with JHOC 7, in which no increase in apoptosis was observed (**Fig. 3D**). ADI-PEG20 treatment decreased colony count of the ASS1-expressing cell line JHOC 7 compared with untreated control, while completely abolishing the clonogenic potential in ASS1-deficient cells (**Fig. 3E**).

To evaluate the enzymatic activity of ASS1 in ovarian cancer cells, we quantified relevant metabolites in ASS1-deficient cell lines (JHOC 5 and COV434), compared with ASS1-proficient cell lines (JHOC 7 and JHOC 9; **Fig. 4A**). Intracellular arginine levels were comparable between all cell lines when cultured in RPMI containing no citrulline. Upon citrulline addition, ASS1-proficient cells exhibited a significant increase in intracellular arginine levels, indicating the utilization of citrulline toward arginine generation. The immediate product of ASS1, argininosuccinate, was not present in ASS1-deficient cell lines even upon addition of citrulline, where a significant increase was seen in ASS1-positive cells in the presence of citrulline. A baseline amount of argininiosuccinate was measured in ASS1-positive cells even without the addition of citrulline, which suggests alternative mechanisms of citrulline generation, such as the nitric oxide pathways. To confirm the specificity of ADI-PEG20 sensitivity to ASS1 expression, we depleted *ASS1* by CRISPR in the ASS1-proficient cell line JHOC7 (**Fig. 4B**). *ASS1* knockout robustly increased the cellular sensitivity to ADI-PEG20. Furthermore, reexpression of ASS1 in JHOC5 rescued its sensitivity to ADI-PEG20 treatment (**Fig. 4C**), further supporting the on-target specificity of ADI-PEG20 in ovarian cancers

SCCOHT is sensitive to ADI-PEG20 *in vivo* in cell line–derived models and patient-derived xenografts

We chose the highly aggressive SCCOHT to assess the efficacy of ADI-PEG20 *in vivo* using two subcutaneous cell line mouse models (COV434 and SCCOHT1) and one patient-derived xenograft mouse model (PDX-465). Once-a-week treatment with ADI-PEG20 (15 mg/kg and 30 mg/kg, equivalent to about 2.5 IU and 5 IU, respectively; refs. 34, 35) for 4 weeks significantly decreased tumor growth compared with control group treated with saline (**Fig. 5A**). The lower dose treatment was very well tolerated. However, with the higher dose (30 mg/kg), we noticed signs of toxicity including weight loss, signs of dehydration and piloerection. Some mice also exhibited enlarged kidneys and livers, but these organs showed no abnormality upon histologic examination (Supplementary Fig. S7A). In the 30 mg/kg treatment group for PDX-465 ($n = 8$), we terminated one subject at day 19 due to excessive weight loss, signs of dehydration, and shallow breathing. Two mice between all treatment groups had infiltrative masses above the heart which were SMARCA4/BRG1 positive (Supplementary Fig. S7B), suggesting the possibility of thymic lymphomas.

In the COV434 model, tumor growth was almost completely blocked by the treatment of 15 mg/kg ADI-PEG20. In the 30 mg/kg group, tumors continuously decreased in size throughout 4 weeks (**Fig. 5A**). By the end of the third week, three tumors in the 30 mg/kg

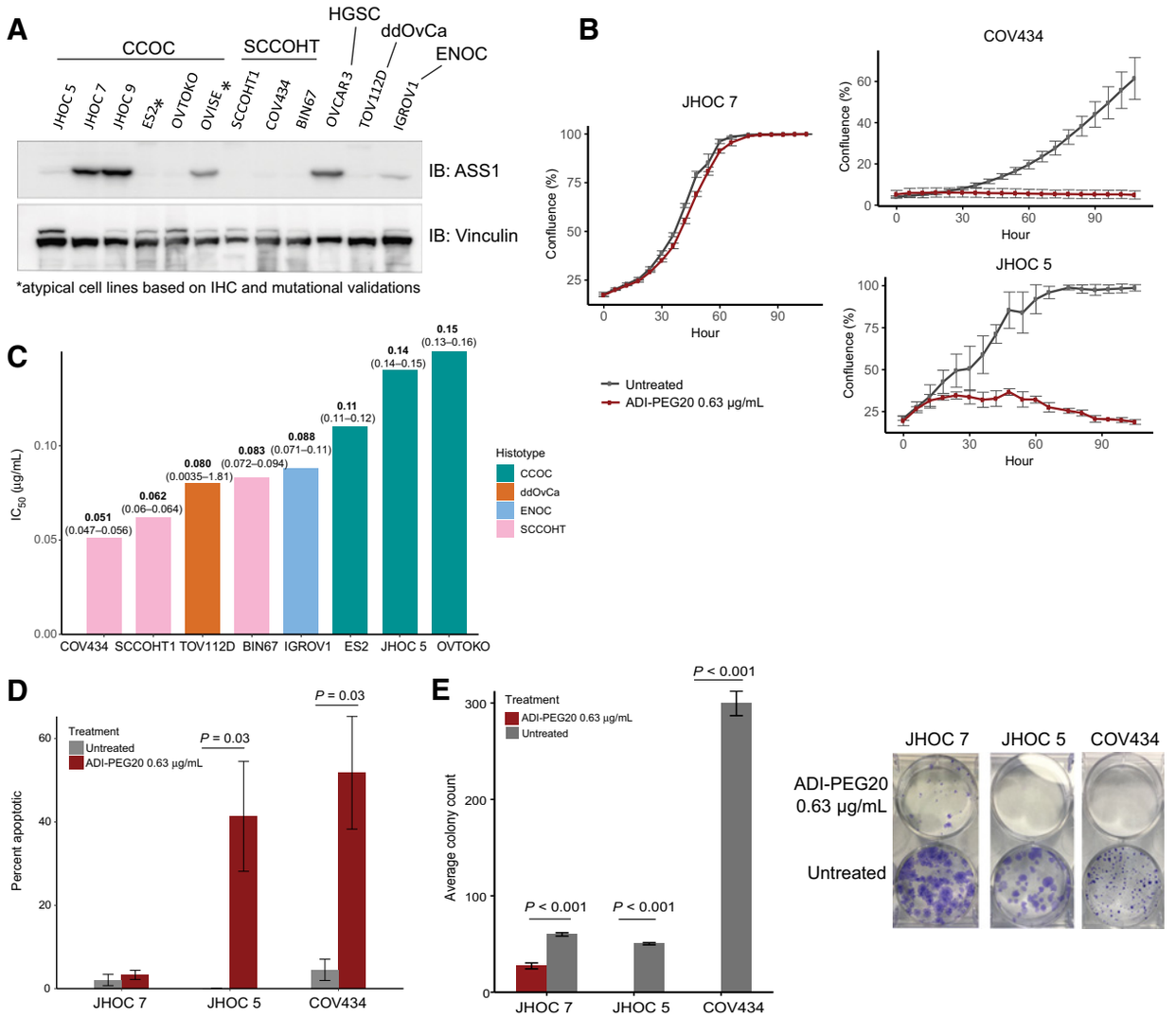

Figure 3.

ASS1-deficient ovarian cancers are sensitive to arginine deprivation through ADI-PEG20. **A,** Western blot analysis showing differential ASS1 expression in representative ovarian cancer cell lines. **B,** Cell proliferation of ASS1-negative SCCOHT cell line (COV434) and CCOC cell line (JHOC 5) compared with ASS1-expressing CCOC cell line (JHOC 7), when treated with 0.63 µg/mL of ADI-PEG20; and bar graph of IC_{50} of ASS1-deficient cell lines representing various ovarian cancer subtypes, IC_{50} (95% confidence interval) are labeled for each cell line (**C**). ASS1-expressing cell lines (JHOC 7, JHOC 9, OVCAR3, OVISE) all had IC_{50} above 2 µg/mL. **D,** Treatment with 0.63 µg/mL of ADI-PEG20 induced apoptosis as shown by a caspase 3/7 cleavage assay in ASS1-deficient, but not in ASS1-expressing cell lines. **E,** ADI-PEG20 treatment abolished the clonogenic potential of ASS1-deficient cell lines, while decreased the clonogenic potential in ASS1-expressing cell line.

group, and one in the 15 mg/kg group were too small to be measured using a caliper. At study termination, the average tumor weight per group in 15 mg/kg and 30 mg/kg dose were 12% and 2.7% of the control group (**Fig. 5B**). In the SCCOHT1 model, 30 mg/kg dose significantly deterred tumor growth over a 3-week treatment period ($P < 0.001$; Supplementary Fig. S7C). However, the tumor weight at termination was not significant for the SCCOHT1 model (Supplementary Fig. S7C). We noticed abundant weak to moderate ASS1 expression in all cases in SCCOHT control and treated groups. The abundance of ASS1 expression in SCCOHT1 control groups was unlike other xenograft models, where ASS1 was absent in the control groups, and could contribute to the lessened effectiveness of ADI-PEG20 (Supplementary Fig. S7D). The identity of the cell line and xenograft was confirmed by the negativity of SMARCA4/BRG1 (Supplementary Fig. S7D). The reexpression of ASS1 *in vivo* in SCCOHT1 could reflect its increased mRNA level compared with other SCCOHT cell lines (Supplementary Fig. S4B).

Upon histologic assessment of COV434 xenograft tumors, tumor morphology recapitulated SCCOHT human tumors and was similar in the treated compared with controlled groups. Mitotic count significantly decreased in both treatment groups compared with control group ($P < 0.001$; **Fig. 5E**). Accordingly, tumors in the treated groups had foci of Ki67 staining where control group exhibited uniformly high Ki67 staining (**Fig. 5D**). Ki67 proliferation index, scored on the basis of

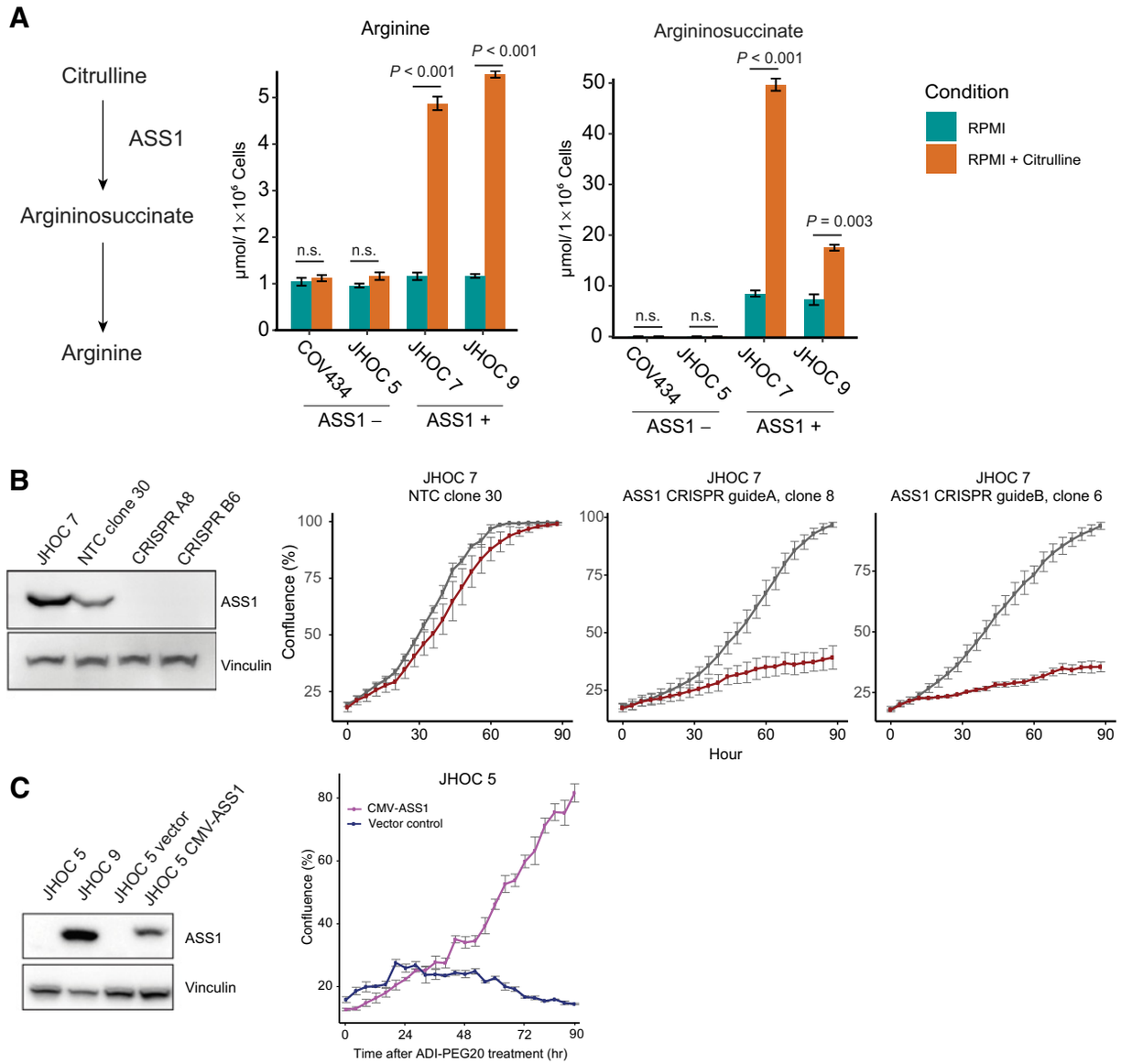

Figure 4.

ASS1 is required for survival in arginine deplete conditions, and its deficiency disrupts urea cycle function. **A,** Argininosuccinate and arginine intracellular measurements in ASS1-deficient cells (JHOC 5 and COV434), compared with ASS1-proficient cells (JHOC 7 and JHOC 9). **B,** Western blot analysis showing the knockout efficiency of two CRISPR *ASS1* knockout clones in a JHOC 7 background (A8: clone 8 using guide A, and B6: clone 6 using guide B, NTC30: empty vector negative control). The specificity of ADI-PEG20 was confirmed in the *ASS1* knockout clones A8 and B6. **C,** Western blot analysis showing the stable overexpression of ASS1 in JHOC 5, rescuing its growth when treated with 0.63 µg/mL of ADI-PEG20. All *P* values were generated from Student *t* test. Error bars, SEM.

the most proliferative areas, was significantly lower in 30 mg/kg group compared with both control and 15 mg/kg groups ($P = 0.003$ and $P = 0.03$, respectively; **Fig. 5F**). However, tumors in the treated groups appeared viable on histology. Tunnel assay also did not show increased apoptosis in the treated tumors compared with controls (Supplementary Fig. S7E). We conducted ASS1 IHC on whole sections of COV434 xenograft tumors. While no tumors expressed ASS1 in the control group, one of seven cases in 30 mg/kg group and two of eight cases in the 15 mg/kg group showed small foci of ASS1 reexpression (Supplementary Fig. S7F), suggesting that SCCOHT cells may regain the expression of ASS1 to develop resistance.

In concordance with our cell line model findings, ADI-PEG20 was effective in controlling tumor growth in a patient-derived xenograft model—PDX-465, both with 30 mg/kg (**Fig. 5A** and **B**), and a dose deescalation of 30 mg/kg to 15 mg/kg (**Fig. 5C**). To ensure the tumor shrinkage was not a result of weight loss associated with toxicity in ADI-PEG20 treatment groups, we graphed the average mouse weight in addition to tumor weight normalized to mouse weight to confirm significant tumor shrinkage in COV434 and PDX465 models (Supplementary Fig S7G and S7H). Collectively, our result suggests ADI-PEG20 can serve as a promising therapy for SCCOHT.

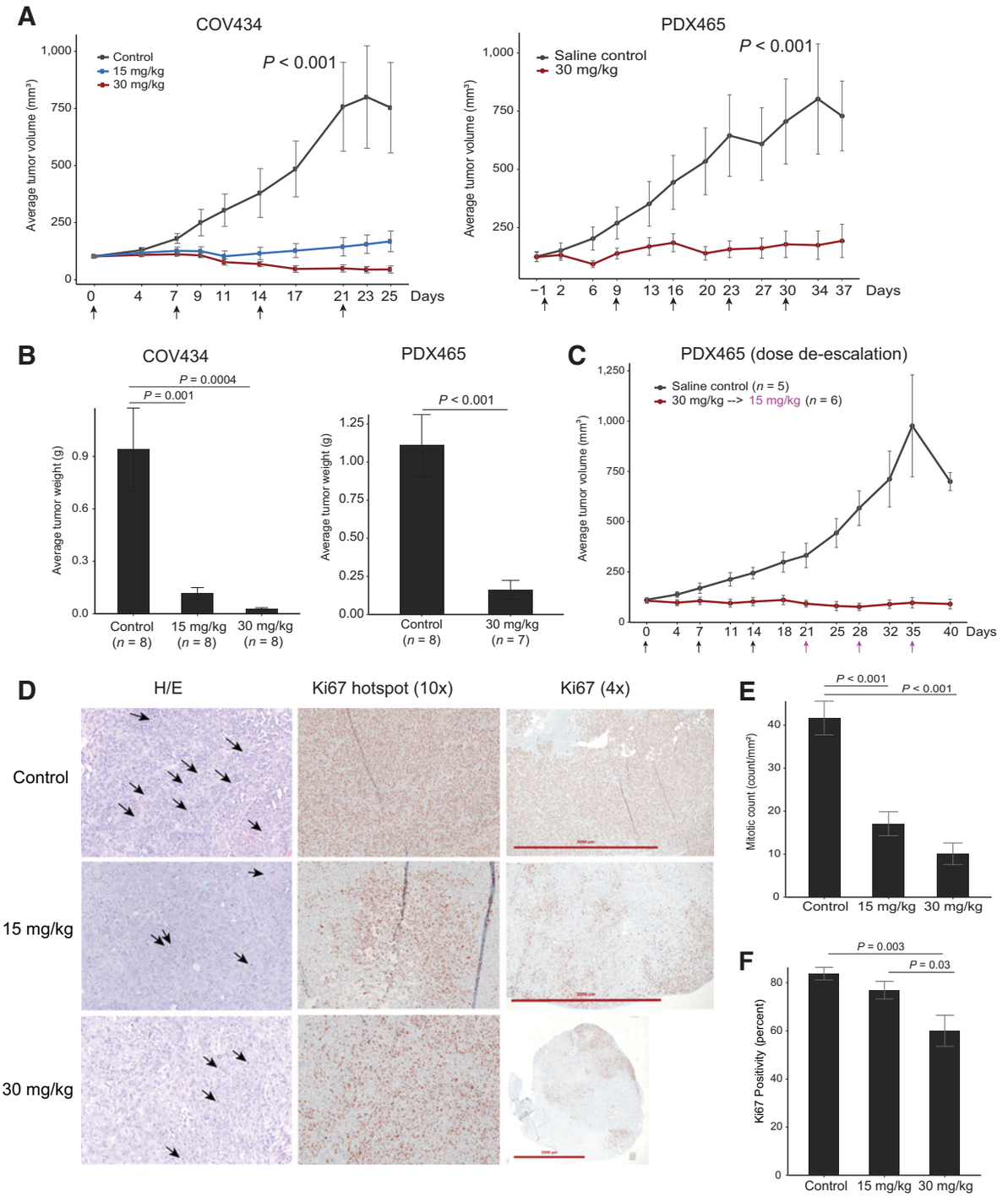

Figure 5.

ADI-PEG20 is effective in inhibiting SCCOHT tumor growth in cell line and patient-derived xenograft based *in vivo* models. **A,** Average tumor volume of the COV434 cell line model and PDX465 patient-derived xenograft model. Mice were treated once a week (indicated by arrows). **B,** Average weight of tumors at study termination. **C,** Average tumor volume of an additional PDX-465 experiment where subjects received 3 weeks of 30 mg/kg (black arrows), followed by 3 weeks of 15 mg/kg (magenta arrows). **D,** Histology and Ki67 IHC of representative tumors from the control and treatment groups from the COV434 model. Ki67 score was determined on the basis of the area with the most intense staining. Arrows represent mitotic figures. **E,** Average mitotic count on whole sections indicating significantly dampened mitotic activity in both treatment groups in the COV434 model. **F,** Average Ki67 score between groups showing significantly decreased proliferation in the 30 mg/kg group in the COV434 model. For multiple group comparisons, significance was calculated using ANOVA, followed by a *post hoc* Tukey test. Error bars, SEM.

Discussion

Effective therapy for rare and aggressive ovarian cancer subtypes is urgently needed, as they still affect thousands of women every year. Like many rare diseases, research efforts and clinical trial options for patients with rare ovarian cancers are limited. In this study, we identified ASS1 deficiency as a common vulnerability among some rare and clinically aggressive ovarian cancer subtypes, supporting the development of a rare tumor–focused clinical trial using ADI-PEG20. ADI-PEG20, a PEGylated form of the bacterial enzyme arginine deiminase, effectively depletes plasma arginine level (23). The agent is currently in phase I to III clinical trials for malignant mesothelioma, melanoma, and hepatocellular cancers, has been designated an orphan drug for malignant mesothelioma in Europe and the United States (36, 37).

The cellular origins of ovarian cancer subtypes have been much debated; HGSC is postulated to arise from abnormal fallopian tube cells, ENOC and CCOC arise from ovarian endometriosis (2), while the cellular origin of SCCOHT remains unknown. The evolving knowledge of a diverse, extraovarian tissue of origin for each subtype poses a challenge in ovarian cancer research especially in comparing tumors with their corresponding normal tissues. In this study, we focus on identifying clinically actionable differences between ovarian cancer subtypes, based on molecular insights, rather than purely on cellular origins or histologic appearance. Using a validated global proteomic approach SP3-CTP (25), we compared rare ovarian cancer subtypes ENOC, CCOC, and SCCOHT with HGSC to identify decreased ASS1 expression in ENOC and CCOC compared with HGSC with confirmation through IHC. In our patient cohort, 15% of ENOC and 72% of CCOC had intense expression of ASS1. While our ENOC results are similar to findings by Cheon and colleagues, only 13% of CCOC had high levels of ASS1 in this previous report (20). This discrepancy could be due to differences in scoring metrics and antibodies used. Our results indicating high ASS1 expression in HGSC cases corroborate with previous proteomic findings in ovarian cancer cell lines (38) and IHC findings in patient tissues (20).

In addition to epithelial ovarian cancers, we expanded our investigation into rare, nonepithelial subtypes. A global proteomics study of an additional six cases of SCCOHT and HGSC identified ASS1 as one of the most significantly differentially expressed proteins. We found universally low ASS1 expression in 31 SCCOHT cases with low heterogeneity across cores taken from different areas of the tumor. In SCCOHT cell lines, we found *ASS1* silencing by promoter methylation in the COV434 and SCCOHT1 lines, but not in BIN67. However, reexpression of SMARCA4 in the cell lines did not restore ASS1 expression. Because SCCOHT possess no mutations beyond the inactivation of SMARCA4, our data suggest that the absence of ASS1 expression may represent an intrinsic feature of cell of origin of SCCOHT. We also saw low ASS1 expression in SLCT and GCT. Although both SLCT and GCT have mostly an indolent disease course, recurrent and metastatic diseases still result in poor outcome (17, 18). We did not have survival information for SLCT and GCT cases included in this study; further correlation between ASS1 expression and clinical parameters should be completed to determine whether ADI-PEG20 could be a therapy for patients diagnosed with aggressive SLCT and GCT.

The IHC survey of ovarian cancer subtypes identified possible responders to ADI-PEG20 treatment, including CCOC, ENOC, GCT, SLCT, and SCCOHT. We then showed that ASS1-deficient ovarian cancer cell lines were sensitive to ADI-PEG20 treatment regardless of subtype. ADI-PEG20 sensitivity in cell lines OVCAR3, ES2, and TOV112D agreed with previous findings (20). In addition, we report promising *in vitro* efficacy of ADI-PEG20 in a panel of CCOC and SCCOHT cell lines, for which both growth and clonogenic potential were inhibited. ADI-PEG20 treatment has previously been shown to cause cell death by apoptosis in leukemia cells (39), but could induce caspase-independent autophagy in prostate cancer cells (40). In our study, ADI-PEG20 was shown to induce ovarian cancer cell death through apoptosis.

Our observation that ASS1 expression correlated with *CTNNB1* mutation in both endometrioid ovarian cancers and endometroid endometrial cancers is curious. Because we did not find this correlation in other *CTNNB1*-driven cancers such as colon adenocarcinoma (TCGA data not shown), this seems to be a gynecologic cancer–specific phenotype. While identifying the mechanism behind this association is beyond the scope of this study, we hope our finding can provide insight into the difficulties in clinical management associated with *CTNNB1* mutations in gynecologic cancers.

In our subcutaneous COV434 mouse model, treatment with 30 mg/-kg (5 IU) of ADI-PEG20 resulted in tumor shrinkage in all eight cases within 3 weeks of treatment, including one complete response. Similarly, both 30 mg/kg and 30 mg/kg to 15 mg/kg dose deescalation in PDX-465 significantly inhibited tumor growth. While overall Ki67 staining and mitotic count decreased in the treated COV434 tumors (**Fig. 5E** and **F**), there were still notable Ki67 foci even in the 30 mg/kg group. The *in vivo* experiments were conducted for a maximum of 6 weeks, most patients will receive multiple cycles of ADI-PEG20, presumably leading to sustained response. Nonetheless, the presence of residual viable tumor at the end of our study suggests that while ADI-PEG20 monotherapy induces a drastic response in SCCOHT, combination therapy may provide additional benefit in this difficult to treat disease. We observed cases with small areas of ASS1 reexpression in COV434 treatment groups, and an abundance of ASS1 expression in the SCCOHT1 model in both control and treated group, leading to therapeutic resistance. Together, these results suggest that therapeutic resistance through ASS1 reexpression could be anticipated in some patients with SCCOHT where *ASS1* is silenced due to promoter methylation. In previous preclinical *in vivo* models, 5 IU of ADI-PEG20 showed efficacy in small-cell lung cancer and pancreatic cancer (34, 35). A recent phase I/IB trial single-arm study combining ADI-PEG20 with paclitaxel and gemcitabine in 18 patients with advanced pancreatic cancer showed minimal toxicity, and an overall response rate of 45% with a disease control rate of 91% (41). The encouraging clinical translation in pancreatic cancer suggests that our *in vivo* results may predict a strong response in the clinical setting for patients with SCCOHT.

To date, ADI-PEG20 has been extensively studied with clinical trials in hepatocellular carcinoma, melanoma, and mesothelioma (31). ADI-PEG20 monotherapy was found to be active in a variety of cancers. Weekly treatment of ADI-PEG20 improved progression-free survival by 1.2 months in patients with refractory, chemoresistant malignant mesothelioma (42). However, response of ADI-PEG20 monotherapy in some clinical setting has shown to be transient, related to the neutralization of the agent by host antibodies, as well as ASS1 reexpression in tumors. Instead, recent clinical trial studies focus on the combination of ADI-PEG20 with conventional chemotherapy to circumvent ADI-PEG20 resistance including studies in mesothelioma (NCT02709512), uveal melanoma (NCT02029690), and soft-tissue sarcomas (NCT03449901). Early clinical activity was seen in prostate cancer and nonsmall-cell lung cancer in a phase I trial combining ADI-PEG20 with docetaxel in advanced tumors (43).

The effectiveness of ADI-PEG20 in aggressive cancers and its favorable side-effect profile in drug combinations inspires confidence in its utility for aggressive and rare ovarian cancers, despite some toxicity observed in our mouse models. Recently for SCCOHT, EZH2 inhibitors and CDK4/6 inhibitors have been identified as potential therapies (13, 16). The EZH2 inhibitor Tazemetostat showed mild clinical activity in SCCOHT, with one of 10 patients sustaining a partial response (44). Our results suggest that ADI-PEG20 could join the forefront of therapeutic development for SCCOHT and could be particularly useful in combination with chemotherapy or other targeted therapeutics. Combined therapy including ADI-PEG20 and immune checkpoint inhibitor in uveal melanoma is being planned (45), and a phase Ib trial combining ADI-PEG20 and pembrolizumab in advanced solid cancers is currently recruiting (NCT03254732). In a recent case report, four patients with SCCOHT were found to respond to anti-PDL1 immune checkpoint inhibitor (46), raising the possibility of combined ADI-PEG20 and checkpoint inhibitors for patients with SCCOHT. In addition to SCCOHT, we noted low or absent ASS1 expression in 10 of 28 (36%) late-stage patients with CCOC. This subset of patients with CCOC may also benefit from such treatment strategies.

Furthermore, recent clinical trials combining ADI-PEG20 with conventional chemotherapy have included ASS1-positive chemotherapy refractory patients, and encouraging results have been observed in gastrointestinal cancers and pancreatic cancers regardless of ASS1 expression (41, 47). This additive efficacy has been proposed to be a result of arginine deprivation–induced metabolic stress sensitizing cancers to DNA-damaging agents in an ASS1-independent manner (41). In our *in vitro* studies, ADI-PEG20 treatment significantly decreased the clonogenic potential in ASS1-expressing CCOC cell line JHOC 7 (**Fig. 3**). This result could indicate that combination of ADI-PEG20 and chemotherapy treatment may benefit patients with late-stage ovarian cancer with or without ASS1 deficiency.

In summary, our results suggest ADI-PEG20 offers a promising therapeutic option for rare and aggressive ovarian cancer subtypes, notably in patients with SCCOHT, whose clinical outcomes are otherwise dismal. Clinical evaluation through a trial focused on gynecologic cancers would be an appropriate next step to determine the utility of this treatment approach.

Disclosure of Potential Conflicts of Interest

No potential conflicts of interest were disclosed.

Authors' Contributions

Conception and design: J.X. Ji, D.R. Cochrane, B.E. Weissman, L. Hoang, P. Pirrotte, Y. Wang, D.G. Huntsman

Development of methodology: J.X. Ji, G. Ho, I.N. Alcazar, S. Colborne, G.B. Morin, P. Pirrotte

Acquisition of data (provided animals, acquired and managed patients, provided facilities, etc.): J.X. Ji, B. Tessier-Cloutier, S.Y. Chen, G. Ho, K.V. Pathak, I.N. Alcazar, S. Leung, S. Colborne, F. Kommoss, A. Karnezis, J.N. McAlpine, C.B. Gilks, P. Pirrotte

Analysis and interpretation of data (e.g., statistical analysis, biostatistics, computational analysis): J.X. Ji, K.V. Pathak, D. Farnell, S. Leung, S. Colborne, G.L. Negri, P. Pirrotte

Writing, review, and/or revision of the manuscript: J.X. Ji, D.R. Cochrane, B. Tessier-Cloutier, K.V. Pathak, A. Karnezis, G.B. Morin, J.N. McAlpine, C.B. Gilks, B.E. Weissman, J.M. Trent, L. Hoang, P. Pirrotte, Y. Wang, D.G. Huntsman

Administrative, technical, or material support (i.e., reporting or organizing data, constructing databases): B. Tessier-Cloutier, A. Cheng, C. Chow, F. Kommoss, G.B. Morin

Study supervision: D.R. Cochrane, C.B. Gilks, L. Hoang, Y. Wang, D.G. Huntsman

Other (pathology review): B. Tessier-Cloutier

Acknowledgments

This research is supported by funds from the Canadian Cancer Society Research Institute's Impact grant no. 705647 (to D.G. Huntsman) and Innovation grant no. 703458 (to D.G. Huntsman, Y. Wang), the NCI of NIH (United States; 1R01CA195670-01, to D.G. Huntsman, Y. Wang, A. Karnezis, B.E. Weissman, J.M. Trent), the Terry Fox Research Institute Initiative New Frontiers Program in Cancer (TFF1021, to D.G. Huntsman), the Canadian Institutes of Health Research Foundation grant no. 154290 (D.G. Huntsman), and the Janet D. Cottrelle Foundation through the BC Cancer Foundation (to D.G. Huntsman). The VGH & UBC Hospital Foundation and the BC Cancer Foundation provided funding to OVCARE: BC's Ovarian Cancer Research Team. J.X. Ji is supported by a Vanier Canada graduate scholarship and UBC-BCCA MD/PhD studentship. D.G. Huntsman is supported by the Dr. Chew Wei Memorial Professorship in Gynecologic Oncology and the Canada Research Chairs program (Research Chair in Molecular and Genomic Pathology). The authors thank Polaris Pharmaceuticals for providing ADI-PEG20 and OVCARE tumor bank for providing patient tissues. The authors also thank Derek Wong, Winnie Yang, Janine Senz, and Amy Lum for their technical support. They thank Michelle Woo for assisting with REB protocols for this study.

The costs of publication of this article were defrayed in part by the payment of page charges. This article must therefore be hereby marked *advertisement* in accordance with 18 U.S.C. Section 1734 solely to indicate this fact.

Received June 16, 2019; revised January 2, 2020; accepted May 11, 2020; published first May 14, 2020.

References

1. Torre LA, Trabert B, DeSantis CE, Miller KD, Samimi G, Runowicz CD, et al. Ovarian cancer statistics, 2018. CA Cancer J Clin 2018;68:284–96.
2. Karnezis AN, Cho KR, Gilks CB, Pearce CL, Huntsman DG. The disparate origins of ovarian cancers: pathogenesis and prevention strategies. Nat Rev Cancer 2017;17:65–74.
3. Pujade-Lauraine E, Ledermann JA, Selle F, Gebski V, Penson RT, Oza AM, et al. Olaparib tablets as maintenance therapy in patients with platinum-sensitive, relapsed ovarian cancer and a BRCA1/2 mutation (SOLO2/ENGOT-Ov21): a double-blind, randomised, placebo-controlled, phase 3 trial. Lancet Oncol 2017;18:1274–84.
4. Wiegand KC, Shah SP, Al-Agha OM, Zhao Y, Tse K, Zeng T, et al. ARID1A mutations in endometriosis-associated ovarian carcinomas. N Engl J Med 2010;363:1532–43.
5. Sato N, Tsunoda H, Nishida M, Morishita Y, Takimoto Y, Kubo T, et al. Loss of heterozygosity on 10q23.3 and mutation of the tumor suppressor gene PTEN in benign endometrial cyst of the ovary: possible sequence progression from benign endometrial cyst to endometrioid carcinoma and clear cell carcinoma of the ovary. Cancer Res 2000;60:7052–6.
6. McConechy MK, Ding J, Senz J, Yang W, Melnyk N, Tone AA, et al. Ovarian and endometrial endometrioid carcinomas have distinct CTNNB1 and PTEN mutation profiles. Mod Pathol 2014;27:128–34.
7. Geisler JP, Goodheart MJ, Sood AK, Holmes RJ, Hatterman-Zogg MA, Buller RE. Mismatch repair gene expression defects contribute to microsatellite instability in ovarian carcinoma. Cancer 2003;98:2199–206.
8. Chan JK, Teoh D, Hu JM, Shin JY, Osann K, Kapp DS. Do clear cell ovarian carcinomas have poorer prognosis compared to other epithelial cell types? A study of 1411 clear cell ovarian cancers. Gynecol Oncol 2008;109:370–6.
9. Chan JK, Brady W, Monk BJ, Brown J, Shahin MS, Rose PG, et al. A phase II evaluation of sunitinib in the treatment of persistent or recurrent clear cell ovarian carcinoma: an NRG oncology/gynecologic oncology group study (GOG-254). Gynecol Oncol 2018;150:247–52.
10. Oda K, Hamanishi J, Matsuo K, Hasegawa K. Genomics to immunotherapy of ovarian clear cell carcinoma: unique opportunities for management. Gynecol Oncol 2018;151:381–9.
11. Estel R, Hackethal A, Kalder M, Münstedt K. Small cell carcinoma of the ovary of the hypercalcaemic type: an analysis of clinical and prognostic aspects of a rare

disease on the basis of cases published in the literature. Arch Gynecol Obstet 2011;284:1277–82.
12. Karnezis AN, Wang Y, Ramos P, Hendricks WPD, Oliva E, D'Angelo E, et al. Dual loss of the SWI/SNF complex ATPases SMARCA4/BRG1 and SMARCA2/BRM is highly sensitive and specific for small cell carcinoma of the ovary, hypercalcaemic type. J Pathol 2016;238:389–400.
13. Wang Y, Chen SY, Karnezis AN, Colborne S, Santos ND, Lang JD, et al. The histone methyltransferase EZH2 is a therapeutic target in small cell carcinoma of the ovary, hypercalcaemic type. J Pathol 2017;242:371–83.
14. Wang Y, Chen SY, Colborne S, Lambert G, Shin CY, Santos ND, et al. Histone deacetylase inhibitors synergize with catalytic inhibitors of EZH2 to exhibit antitumor activity in small cell carcinoma of the ovary, hypercalcemic type. Mol Cancer Ther 2018;17:2767–79.
15. Lang JD, Hendricks WPD, Orlando KA, Yin H, Kiefer J, Ramos P, et al. Ponatinib shows potent antitumor activity in small cell carcinoma of the ovary hypercalcemic type (SCCOHT) through multikinase inhibition. Clin Cancer Res 2018;24:1932–43.
16. Xue Y, Meehan B, Macdonald E, Venneti S, Wang XQD, Witkowski L, et al. CDK4/6 inhibitors target SMARCA4-determined cyclin D1 deficiency in hypercalcemic small cell carcinoma of the ovary. Nat Commun 2019;10:558.
17. Young RH, Scully RE. Ovarian sertoli-leydig cell tumors. a clinicopathological analysis of 207 cases. Am J Surg Pathol 1985;9:543–69.
18. Khosla D, Dimri K, Pandey AK, Mahajan R, Trehan R. Ovarian granulosa cell tumor: clinical features, treatment, outcome, and prognostic factors. N Am J Med Sci 2014;6:133–8.
19. Nicholson LJ, Smith PR, Hiller L, Szlosarek PW, Kimberley C, Sehouli J, et al. Epigenetic silencing of argininosuccinate synthetase confers resistance to platinum-induced cell death but collateral sensitivity to arginine auxotrophy in ovarian cancer. Int J Cancer 2009;125:1454–63.
20. Cheon DJ, Walts AE, Beach JA, Lester J, Bomalaski JS, Walsh CS, et al. Differential expression of argininosuccinate synthetase in serous and non-serous ovarian carcinomas. J Pathol Clin Res 2015;1:41–53.
21. Haines RJ, Pendleton LC, Eichler DC. Argininosuccinate synthase: at the center of arginine metabolism. Int J Biochem Mol Biol 2011;2:8–23.
22. Qiu F, Huang J, Sui M. Targeting arginine metabolism pathway to treat arginine-dependent cancers. Cancer Lett 2015;364:1–7.
23. Holtsberg FW, Ensor CM, Steiner MR, Bomalaski JS, Clark MA. Poly(ethylene glycol) (PEG) conjugated arginine deiminase: effects of PEG formulations on its pharmacological properties. J Control Release 2002;80:259–71.
24. Otte A, Gohring G, Steinemann D, Schlegelberger B, Groos S, Langer F, et al. A tumor-derived population (SCCOHT-1) as cellular model for a small cell ovarian carcinoma of the hypercalcemic type. Int J Oncol 2012;41:765–75.
25. Hughes CS, McConechy MK, Cochrane DR, Nazeran T, Karnezis AN, Huntsman DG, et al. Quantitative profiling of single formalin fixed tumour sections: proteomics for translational research. Sci Rep 2016;6:34949.
26. Kommoss S, Anglesio MS, Mackenzie R, Yang W, Senz J, Ho J, et al. FOXL2 molecular testing in ovarian neoplasms: diagnostic approach and procedural guidelines. Mod Pathol 2013;26:860–7.
27. Kalloger SE, Kobel M, Leung S, Mehl E, Gao D, Marcon KM, et al. Calculator for ovarian carcinoma subtype prediction. Mod Pathol 2011;24:512–21.
28. Ramos P, Karnezis AN, Craig DW, Sekulic A, Russell ML, Hendricks WP, et al. Small cell carcinoma of the ovary, hypercalcemic type, displays frequent inactivating germline and somatic mutations in SMARCA4. Nat Genet 2014;46:427–9.
29. Talhouk A, McConechy MK, Leung S, Yang W, Lum A, Senz J, et al. Confirmation of ProMisE: a simple, genomics-based clinical classifier for endometrial cancer. Cancer 2017;123:802–13.
30. Wang YK, Bashashati A, Anglesio MS, Cochrane DR, Grewal DS, Ha G, et al. Genomic consequences of aberrant DNA repair mechanisms stratify ovarian cancer histotypes. Nat Genet 2017;49:856–65.
31. Keshet R, Szlosarek P, Carracedo A, Erez A. Rewiring urea cycle metabolism in cancer to support anabolism. Nat Rev Cancer 2018;18:634–45.
32. NIH. ClinicalTrials.gov. Available from: https://clinicaltrials.gov/ct2/results?cond=&term=adi-peg&cntry=&state=&city=&dist=.
33. Delage B, Luong P, Maharaj L, O'Riain C, Syed N, Crook T, et al. Promoter methylation of argininosuccinate synthetase-1 sensitises lymphomas to arginine deiminase treatment, autophagy and caspase-dependent apoptosis. Cell Death Dis 2012;3:e342.
34. Kelly MP, Jungbluth AA, Wu BW, Bomalaski J, Old LJ, Ritter G. Arginine deiminase PEG20 inhibits growth of small cell lung cancers lacking expression of argininosuccinate synthetase. Br J Cancer 2012;106:324–32.
35. Bowles TL, Kim R, Galante J, Parsons CM, Virudachalam S, Kung HJ, et al. Pancreatic cancer cell lines deficient in argininosuccinate synthetase are sensitive to arginine deprivation by arginine deiminase. Int J Cancer 2008;123:1950–5.
36. U.S. Food and Drug Administration. Search orphan drug designations and approvals. Available from: https://www.accessdata.fda.gov/scripts/opdlisting/oopd/detailedIndex.cfm?cfgridkey=437014.
37. European Medicines Agency. Public summary of opinion on orphan designation. Available from: https://www.ema.europa.eu/en/documents/orphan-designation/eu/3/14/1409-public-summary-opinion-orphan-designation-pegylated-recombinant-arginine-deiminase-treatment_en.pdf.
38. Coscia F, Watters KM, Curtis M, Eckert MA, Chiang CY, Tyanova S, et al. Integrative proteomic profiling of ovarian cancer cell lines reveals precursor cell associated proteins and functional status. Nat Commun 2016;7:12645.
39. Gong H, Zolzer F, von Recklinghausen G, Havers W, Schweigerer L. Arginine deiminase inhibits proliferation of human leukemia cells more potently than asparaginase by inducing cell cycle arrest and apoptosis. Leukemia 2000;14:826–9.
40. Kim RH, Coates JM, Bowles TL, McNerney GP, Sutcliffe J, Jung JU, et al. Arginine deiminase as a novel therapy for prostate cancer induces autophagy and caspase-independent apoptosis. Cancer Res 2009;69:700–8.
41. Lowery MA, Yu KH, Kelsen DP, Harding JJ, Bomalaski JS, Glassman DC, et al. A phase 1/1B trial of ADI-PEG 20 plus nab-paclitaxel and gemcitabine in patients with advanced pancreatic adenocarcinoma. Cancer 2017;123:4556–65.
42. Szlosarek PW, Steele JP, Nolan L, Gilligan D, Taylor P, Spicer J, et al. Arginine deprivation with pegylated arginine deiminase in patients with argininosuccinate synthetase 1-deficient malignant pleural mesothelioma: a randomized clinical trial. JAMA Oncol 2017;3:58–66.
43. Tomlinson BK, Thomson JA, Bomalaski JS, Diaz M, Akande T, Mahaffey N, et al. Phase I trial of arginine deprivation therapy with ADI-PEG 20 plus docetaxel in patients with advanced malignant solid tumors. Clin Cancer Res 2015;21:2480–6.
44. Jones RL, Blay J-Y, Agulnik M, Chugh R, Mir O, Italiano A, et al. A phase II, multicenter study of the EZH2 inhibitor tazemetostat in adults (rhabdoid tumor cohort) (NCT02601950). Ann Oncol 2018;29 Suppl 8:viii580–1.
45. Chan PY, Melissa MP, Khadeir R, Ellis S, Thomson J, Johnston A, et al. Phase 1 study of pegargiminase combined with cisplatin and pemetrexed in patients with ASS1-deficient uveal melanoma. J Clin Oncol 36:15s, 2018 (suppl; abstr 2589).
46. Jelinic P, Ricca J, Van Oudenhove E, Olvera N, Merghoub T, Levine DA, et al. Immune-active microenvironment in small cell carcinoma of the ovary, hypercalcemic type: rationale for immune checkpoint blockade. J Natl Cancer Inst 2018;110:787–90.
47. Harding JJ, Do RK, Dika IE, Hollywood E, Uhlitskykh K, Valentino E, et al. A phase 1 study of ADI-PEG 20 and modified FOLFOX6 in patients with advanced hepatocellular carcinoma and other gastrointestinal malignancies. Cancer Chemother Pharmacol 2018;82:429–40.